

Electronic Supplementary Information:

Design Principles of Tandem Cascade Photoelectrochemical Devices

Calton J. Kong,^{†,#} Emily L. Warren,[¶] Ann L. Greenaway,[¶]

Rajiv Ramanujam Prabhakar,^{†,#} Adele C. Tamboli,[¶] and Joel W. Ager^{†,‡,Δ}

[†]Liquid Sunlight Alliance, [#]Chemical Sciences Division, [‡]Materials Sciences Division, Lawrence
Berkeley National Laboratory, California 94720, United States

^ΔDepartment of Materials Science and Engineering, University of California, Berkeley,
California 94720, United States

[¶]Liquid Sunlight Alliance, National Renewable Energy Laboratory, Golden, Colorado 80401,
United States

Table of Contents

Simulation Methods	2
Supplemental data	2
Supplemental References	11

SIMULATION METHODS

Circuit simulations were performed with Ngspice using the Python interface PySpice.^{1,2} Some aspects of circuit design were performed using LTSpice.³ PV elements were modeled as a diode situated in parallel to a current source, excluding any impact from non-ideal shunt or series resistances. Catalysts were modeled as voltage-controlled non-linear current sources. Details and example netlists are in Jupyter notebooks which will be available on Github or an equivalent publicly accessible repository.

SUPPLEMENTAL DATA

Table S1: Previously reported 2J-2T devices used for PEC CO₂R.

PV Elements	Product(s)	FE	Solar to Fuel Efficiency
GaInP/GaAs	HCOO ⁻	94%	10% ⁸
Halide Perovskite/Si	C ₂₊ mix	Mix	1.5% ⁹

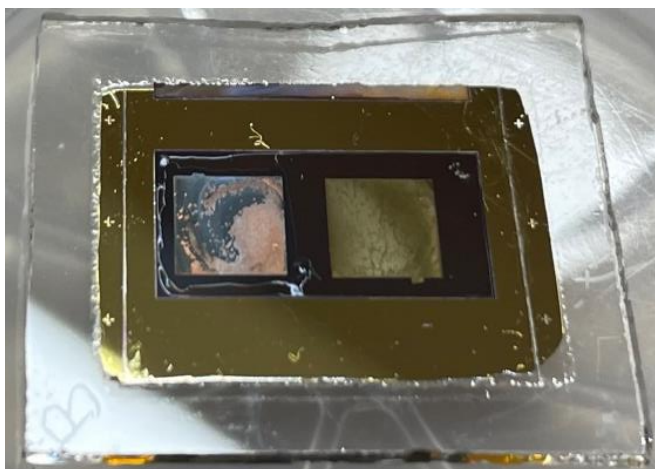


Figure S1: Prototype 3TT cell with copper and gold catalysts on the R and Z contact. This type of device could be used to realize the concepts discussed in this paper.

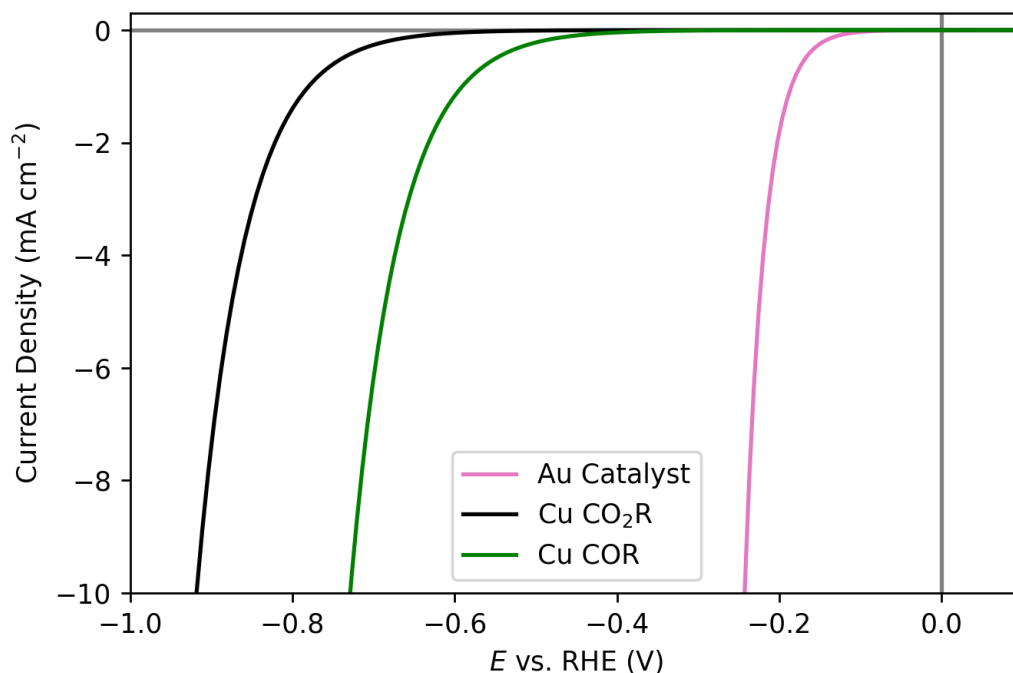


Figure S2: Current model for the catalysts used in the simulation. Data for Au and COR synthesized from exchange current and Tafel slopes from Li *et al.*,⁴ Jouny *et al.*,⁵ and Chen *et al.*⁶ Representative exchange current densities were taken from Li and Chen, and Tafel data for Cu was taken from Jouny. CO₂R data synthesized from data from Gurudayal *et al.*⁷ These parameters were placed into a Butler Volmer model, to generate the two curves. These curves represent total current densities, faradaic efficiencies are listed in Table 1 of the main document. The current densities used in the simulations map onto experiments performed in near-neutral pH in CO₂-saturated water. We define the onset as that required to produce a current density of 0.1 mA cm⁻²; here, for Cu and Au these values are -0.65 V (CO₂R), -0.45 V (COR), and -0.15 V vs RHE, respectively.

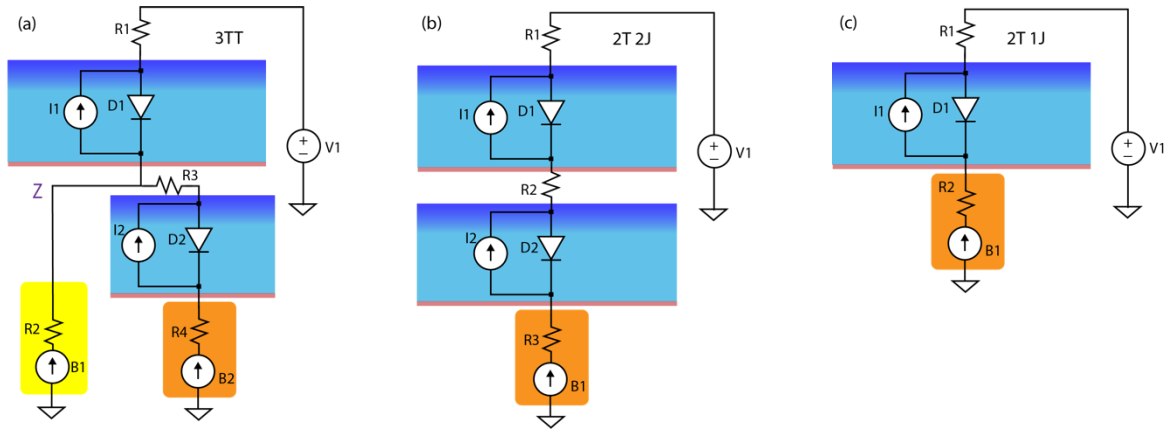


Figure S3: (a) Schematic of equivalent circuit for the three terminal tandem cell used in SPICE simulation. In the diagram the PV elements are the current source and the diode, the reverse saturation current of D1 (GaInP) and D2 (GaAs) were adjusted to produce an open circuit voltage of 1.4 V for GaInP and 1.0 V for GaAs with j_{sc} being 12 mA cm^{-2} . B1 and B2 are non-linear voltage-controlled current sources meant to represent the Au and Cu catalysts, respectively. (b) Schematic of equivalent circuit for the two terminal two junction cell used in SPICE simulation. In the diagram the PV components are the same as (a), but B1 represents the Cu catalyst. (c) Schematic of equivalent circuit used for the two terminal one junction cell used in SPICE simulation. D1 represents the GaInP absorber.

Table S2: Summary of parameters used in the base case SPICE model to the GaInP and GaAs PV elements

GaInP	Model Parameter	GaAs	Model Parameter
I1	-12 mA	I2	-7.5 mA
D1	$I_s = 0.02 \text{ pA}$; $n=2$; $R_s = 0 \text{ Ohm}$	D2	$I_s = 64 \text{ pA}$; $n = 2$; $R_s = 0 \text{ Ohm}$
R1	0 Ohm	R2	0 Ohm

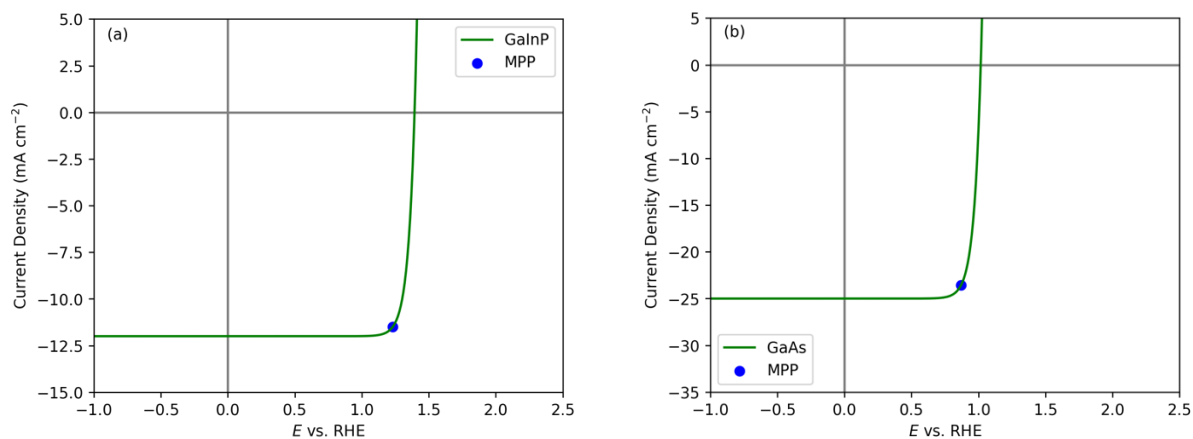


Figure S4: *J-V* behavior of the PV elements used in the cells under 1 sun. (a) Behavior of the GaInP cell. FF = 0.88 (b) Behavior of the GaAs cell as a bottom cell with GaInP on top. FF = 0.85

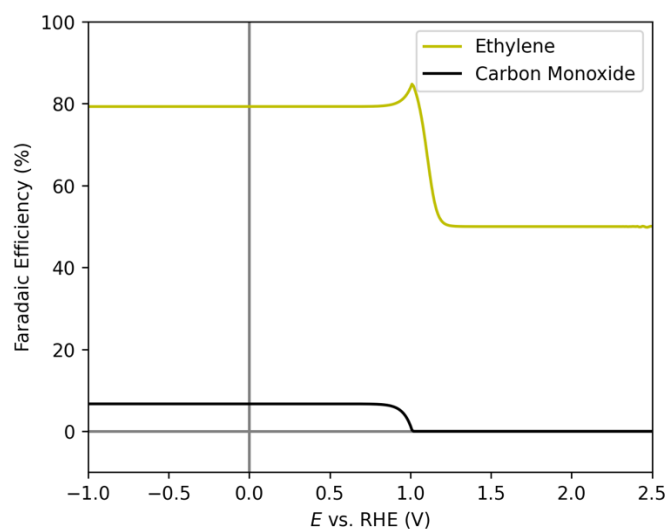


Figure S5: The faradaic efficiencies toward CO and ethylene as a function of the bias for a three-terminal tandem (3TT) photoelectrochemical device, with the circuit shown in Figure S1a. The parameters for this simulation are shown in Table 1 in the main text.

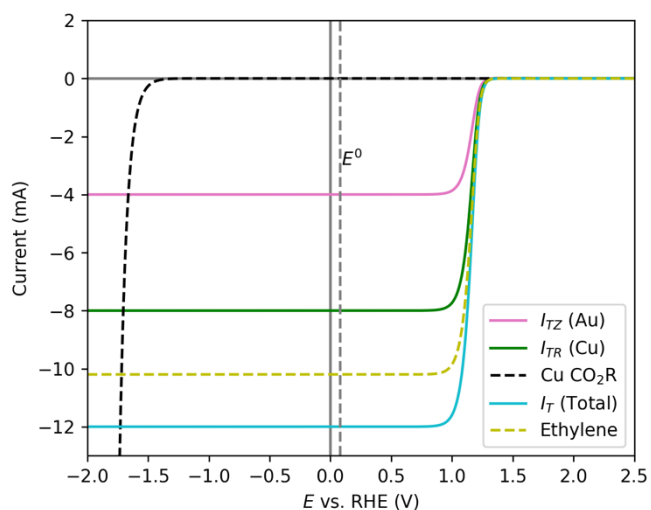


Figure S6: J - V behavior for a cell where the overpotential of CO_2R is far higher than COR, and the area of the GaAs cell causes its short circuit current to exceed 8 mA. Here we set it 10 mA.

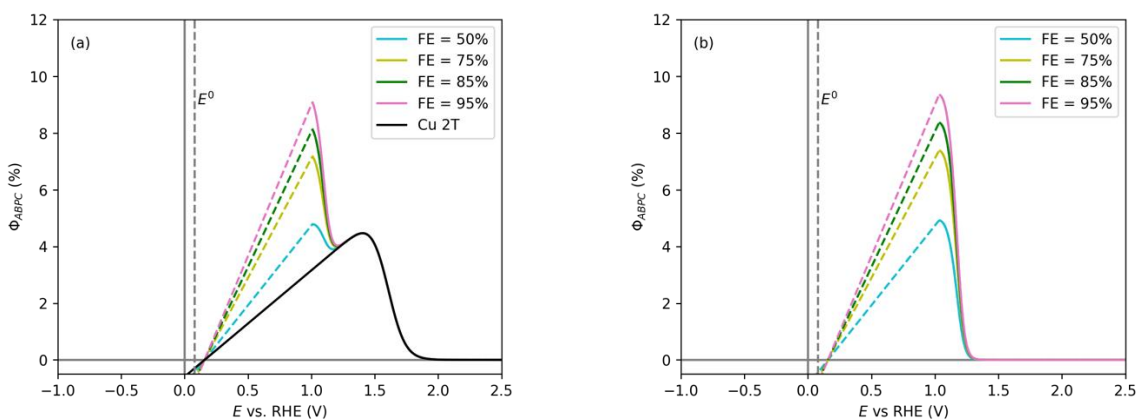


Figure S7: (a) Φ_{ABPC} vs E for the 3TT device when COR and CO_2R have the same activity. Using baseline onset of (-0.45 V) as shown in Table 1 in the main text. (b) Φ_{ABPC} vs E for the 3TT device when the activity for CO_2R is far lower than COR. J - V curves for these two systems are in the main text.

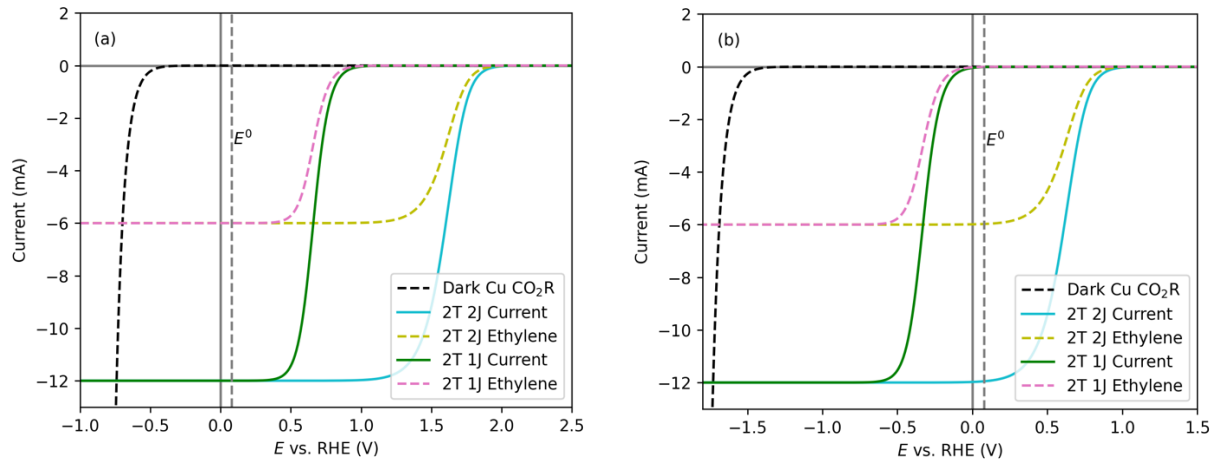
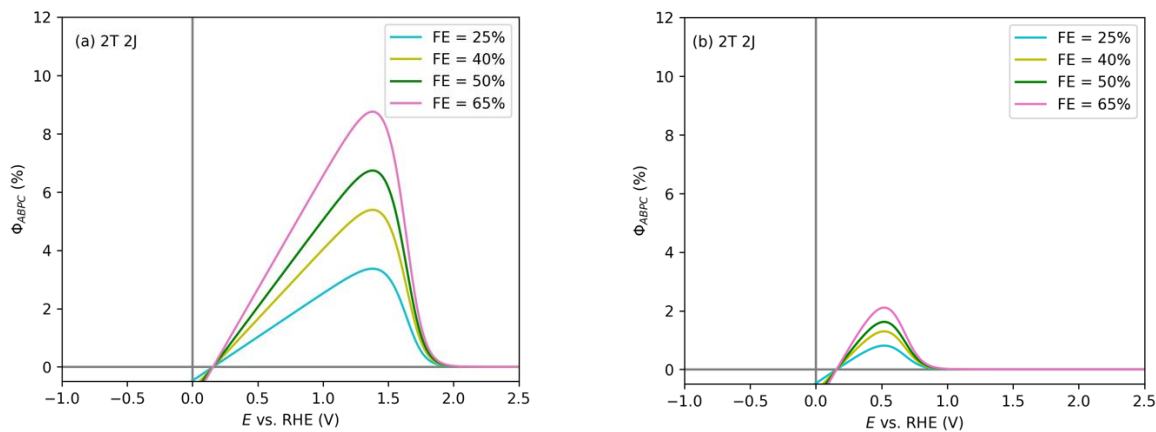


Figure S8: (a) J - V curve for the two terminal two junction (2T 2J) and two terminal one junction (2T 1J) devices when the activity for CO_2R is the same as COR (onset of -0.45 V) as shown in Table 1 in the main text. (b) J - V curve for 2T 2J and 2T 1J devices when the activity for CO_2R is far less than for COR.



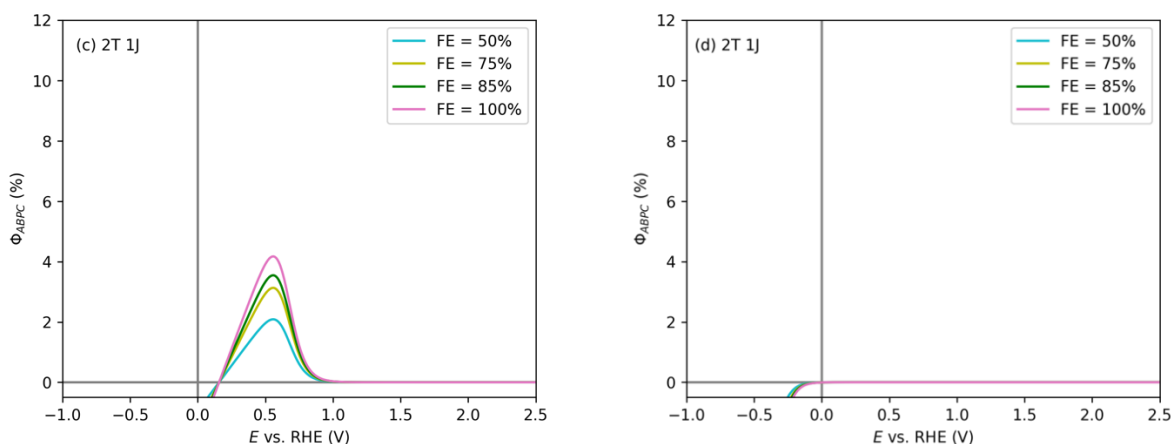


Figure S9: (a) Φ_{ABPC} vs E for the 2T 2 J device when the activity for CO_2R is the same as COR, with parameters shown in Table 1 in the main text. (b) Φ_{ABPC} vs E for the 2T 2J device when the activity for CO_2R is far lower than COR, dark curve shown in Figure S6b. (c) Φ_{ABPC} vs E for the 2T 1J device when the activity for CO_2R is the same as COR, with parameters shown in Table 1 in the main text. (d) Φ_{ABPC} vs E for the 2T 1J device when the activity for CO_2R is far lower than COR, dark curve shown in Figure S6b.

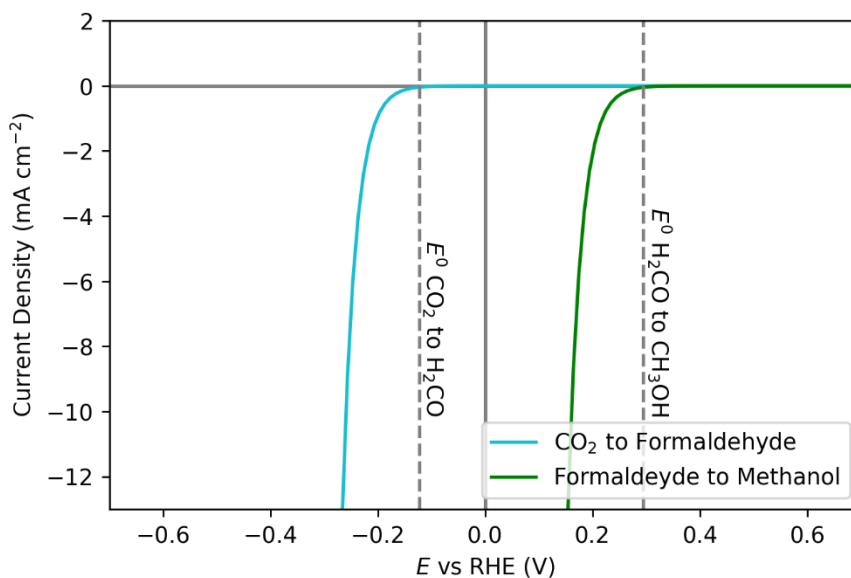


Figure S10: Dark models used for the enzyme catalysts. Modeled to have low overpotential compared to their respective E^0 s.

Table S3: Summary of parameters and properties used to simulate the 3TT enzyme cell in Figure 8a in the main text

(Sub)Cell	J_{sc} (mA cm ⁻²)	V_{oc} (V)	FE (%)	Dark Onset (V)
GaInP/Au	12	1.4	CH ₃ OH: 100	0.25
GaAs/Cu	7.5	1.0	H ₂ CO: 100	-0.15

Table S4: Summary of parameters and properties used to simulate the 3TT enzyme cell in Figure 8b in the main text.

(Sub)Cell	J_{sc} (mA cm ⁻²)	V_{oc} (V)	FE (%)	Dark Onset (V)
GaInP/Au	12	1.4	H ₂ CO: 100	-0.15
GaAs/Cu	3.5	1.0	CH ₃ OH: 100	0.25

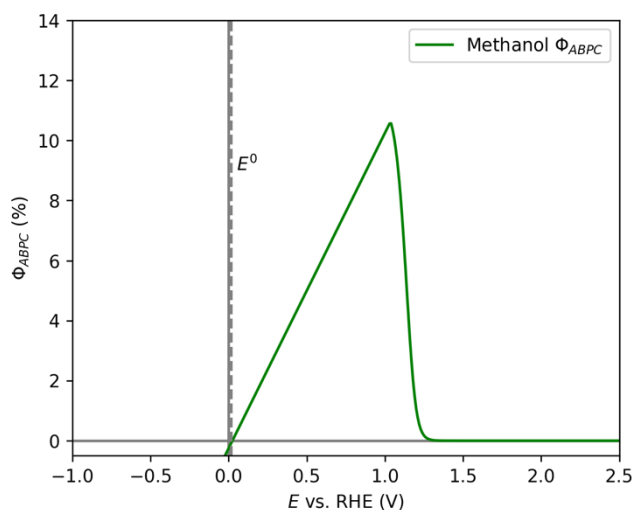


Figure S11: Φ_{ABPC} vs E for the 3TT enzyme system to methanol, with the parameters of the simulation shown in Table S1.

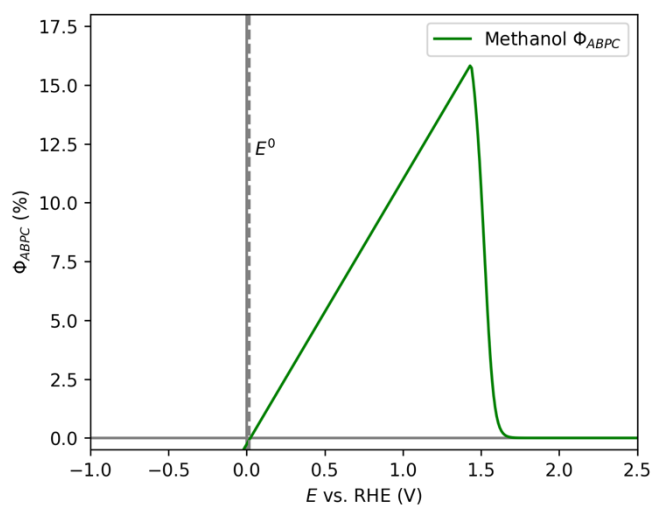


Figure S12: Φ_{ABPC} vs E for the 3TT enzyme system to methanol, with the parameters of the simulation shown in Table S2.

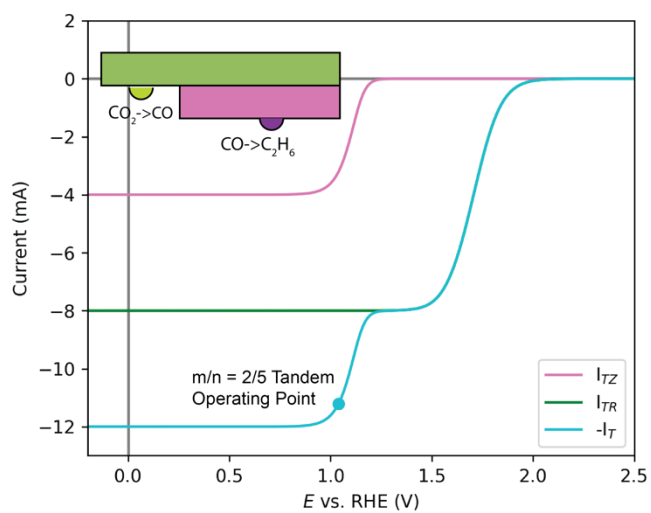


Figure S13: J - V curve for a system driving CO_2 to CO and then to ethane. The inset shows how the relative area of the GaAs needs to increase to accommodate a reaction where $m/n = 2/5$. Parameters of simulation were assuming the same CO dark current (Figure S2), and that CO_2R and COR had the same dark onset of -0.45 V.

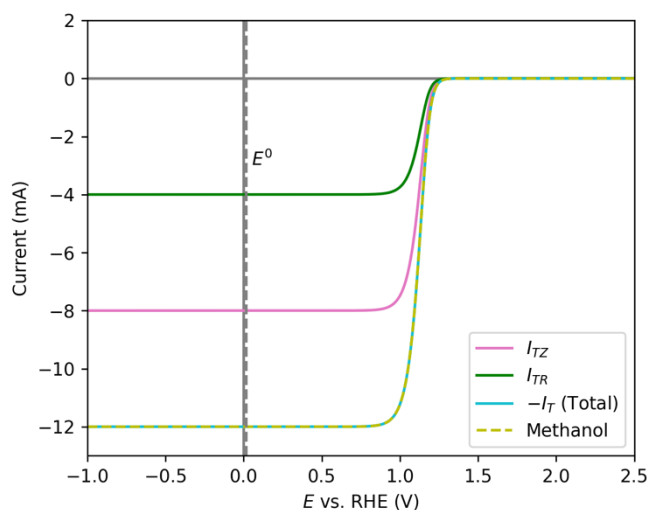


Figure S14: *J-V* curve of the enzyme system where the formaldehyde catalyst was coupled to the GaInP cell and the GaAs cell had an I_{sc2} greater than 4 mA. Just like the case examined where CO₂R was effectively suppressed in the tandem and the ethylene production was limited by the intermediate current, if the area of the GaAs cell was made too large, there wouldn't be enough formaldehyde intermediate for the second enzyme to reduce, hence the limiting currents for the subcells would be 8 mA and 4 mA respectively.

SUPPLEMENTAL REFERENCES

- (1) Vogt, H.; Hendrix, M.; Nenzi, P. NGSPICE, Mixed mode - mixed level circuit simulator <http://ngspice.sourceforge.net>.
- (2) Salvaire, F. PySpice <https://pyspice.fabrice-salvaire.fr>.
- (3) LTSpice <https://www.analog.com/en/design-center/design-tools-and-calculators/ltspice-simulator.html>.
- (4) Li, C. W.; Ciston, J.; Kanan, M. W. Electroreduction of Carbon Monoxide to Liquid Fuel on Oxide-Derived Nanocrystalline Copper. *Nature* **2014**, *508* (7497), 504–507. <https://doi.org/10.1038/nature13249>.
- (5) Jouny, M.; Luc, W.; Jiao, F. High-Rate Electroreduction of Carbon Monoxide to Multi-Carbon Products. *Nat. Catal.* **2018**, *1* (10), 748–755. <https://doi.org/10.1038/s41929-018-0133-2>.
- (6) Chen, Y.; Li, C. W.; Kanan, M. W. Aqueous CO₂ Reduction at Very Low Overpotential on Oxide-Derived Au Nanoparticles. *J. Am. Chem. Soc.* **2012**, *134* (49), 19969–19972. <https://doi.org/10.1021/ja309317u>.
- (7) Gurudayal, G.; Bullock, J.; Srankó, D. F.; Towle, C. M.; Lum, Y.; Hettick, M.; Scott, M.

- C.; Javey, A.; Ager, J. Efficient Solar-Driven Electrochemical CO₂ Reduction to Hydrocarbons and Oxygenates. *Energy Environ. Sci.* **2017**, *10* (10), 2222–2230. <https://doi.org/10.1039/C7EE01764B>.
- (8) Zhou, X.; Liu, R.; Sun, K.; Chen, Y.; Verlage, E.; Francis, S. A.; Lewis, N. S.; Xiang, C. Solar-Driven Reduction of 1 Atm of CO₂ to Formate at 10% Energy-Conversion Efficiency by Use of a TiO₂-Protected III–V Tandem Photoanode in Conjunction with a Bipolar Membrane and a Pd/C Cathode. *ACS Energy Lett.* **2016**, *1* (4), 764–770. <https://doi.org/10.1021/acsenergylett.6b00317>.
- (9) Gurudayal, G.; Beeman, J. W.; Bullock, J.; Wang, H.; Eichhorn, J.; Towle, C.; Javey, A.; Toma, F. M.; Mathews, N.; Ager, J. W. Si Photocathode with Ag-Supported Dendritic Cu Catalyst for CO₂ Reduction. *Energy Environ. Sci.* **2019**, *12* (3), 1068–1077. <https://doi.org/10.1039/C8EE03547D>.